Microneedle-based precision payload delivery in plants

Mingzhuo Li[1], Aditi Dey Poonam[1], Deepjyoti Singh[2], Anna E. Whitfield[2,3], and Qingshan Wei[1,3]*

1. Department of Chemical and Biomolecular Engineering, North Carolina State University, Raleigh, NC 27695
2. Department of Entomology and Plant Pathology, North Carolina State University, Raleigh, NC, 27606
3. Emerging Plant Disease and Global Food Security cluster, North Carolina State University, Raleigh, NC 27695

* Corresponding email: qwei3@ncsu.edu

Running title: **Precision molecular delivery to live plants with microneedles**

Keywords: plant delivery, microneedle, phytohormone, pathogen resistance, precision agriculture

Abstract:

Traditional crop delivery methods, such as foliar spray and soil application, face significant limitations including nutrient loss, environmental impacts, and low delivery efficiency. Recent advances in nanomaterials have offered novel molecular delivery platforms, but challenges such as toxicity, complexity, and labor-intensive processes persist. To address these issues, we developed a polyvinyl alcohol (PVA)-based microneedle (MN) delivery system that can be precisely applied to various plant tissues (e.g., leaves or stems), which demonstrates high delivery efficiency compared to the conventional methods while reducing application dose by 90-99%. This MN system facilitates delivery of diverse small molecules, ranging from fluorescent dyes, growth promoters, to antiviral agents, into plant tissues. By applying fluorescent dye-loaded MNs onto tomato stems, we demonstrated effective molecular diffusion through vascular tissues. Additionally, MNs loaded with gibberellic acid (GA3) enhanced stem and branch growth in tomatoes and restored the lateral flowering phenotype in *Arabidopsis ft-10* mutants, with significant upregulation of GA receptor gene expression. Lastly, salicylic acid (SA) injections with MNs induced resistance to tomato spotted wilt virus (TSWV) in *Nicotiana benthamiana*, comparable to conventional spray and infiltration-based approaches. This easily fabricated and cost-effective PVA-MN system provides a promising tool for precision agriculture, enhancing plant health and productivity while addressing the limitations of conventional delivery methods.

Keywords: plant delivery, microneedle, phytohormone, pathogen resistance, precision agriculture

53 **Introduction:**

54 Currently, two of the most widely used methods for active delivery in agriculture are foliar spray
55 and soil application (Niu *et al.*, 2021, Nkebiwe *et al.*, 2016). These two methods are popular due
56 to their simplicity, speed, and ease of scaling up. However, with the ongoing development of the
57 agricultural industry, significant limitations of these traditional delivery methods have become
58 apparent (Sinha *et al.*, 2022, Zheng *et al.*, 2020). As larger areas of cropland and a wider variety
59 of crops are integrated into the agricultural industry to meet the increasing food demands driven
60 by rapid population growth, these methods of conventional compound application face new
61 challenges (Davis *et al.*, 2016, Fukase & Martin, 2020).

62 The first limitation is nutrient loss. In the foliar spray method, as much as 70% of the
63 chemicals are lost during the application process (Niu et al., 2021, Ishfaq *et al.*, 2022). While the
64 soil application saves more chemicals or nutrients, it still loses nearly 10% to 30% through this
65 method (Pahalvi *et al.*, 2021, Yahaya *et al.*, 2023) due to numerous factors such as leaching, runoff,
66 or volatilization. Another major concern is the impact on the environment. In the foliar spray
67 methods, most of the chemicals may quickly run off into the atmosphere (Niu et al., 2021, Tyagi
68 *et al.*, 2022) or be washed away by rain, leading to environmental pollution. Large amounts of
69 chemicals applied to the soil can result in water contamination, soil acidification, salinization, and
70 negative impacts on soil biodiversity (Young *et al.*, 2021, Brichi *et al.*, 2023, Alkharabsheh *et al.*,
71 2021). The leaf cuticle serves as another barrier for some foliar sprays because it slows down
72 nutrient and chemical absorption (Krishnasree *et al.*, 2021, Vasundhara & Chhabra, 2021, Barłóg
73 *et al.*, 2022). This method also often provides only short-term relief from nutrient deficiencies and
74 needs to be repeated more frequently. Similarly, soil applications are low efficient because of the
75 slow plant responses, as the nutrients need to move through the soil profile before being absorbed
76 by the roots (Barłóg et al., 2022, Dimkpa *et al.*, 2020).

77 In recent years, several approaches have been developed to address those limitations in
78 traditional crop delivery systems to make molecular delivery in plants more effective, optimize
79 resource utilization, and minimize environmental impact. One example of emerging technologies
80 is the use of nanomaterials as plant delivery systems (Salama *et al.*, 2021, Liu *et al.*, 2021, Jakhar
81 *et al.*, 2022, Beig *et al.*, 2022). Nanomaterials show characteristics that protect labile compounds
82 from fast degradation, increase the adhesion of payloads to plants, control the release of payloads,

83 and enhance the permeability of payloads through cuticle or internalization into plant tissues or
84 cells (Nair *et al.*, 2010, Cunningham *et al.*, 2018). For example, nanocarriers (e.g., carbon
85 nanotubes, quantum dots, and metal/metal oxide NPs) are designed to delivery DNA molecules to
86 perform plant genome engineering, such as gene transformation, si-RNA silencing, and gene
87 editing (Cunningham et al., 2018, Nair et al., 2010, Wang *et al.*, 2021, Zhang *et al.*, 2021, Zhang
88 *et al.*, 2022, Zhang *et al.*, 2020). However, most of these genetic molecular delivery methods based
89 on the nanoparticles are limited by the complex nanomaterials design. In addition, toxicity of
90 nanoparticles to plants and animals is still a big concern (Cunningham et al., 2018). Furthermore,
91 these methods are also commonly applied by spraying, which suffer from the method-associated
92 low uptake efficiency (~0.1% for root application and <30% via leaf) (Tudi *et al.*, 2021).
93 Alternative delivery methods such as foliar infiltration are labor-intensive and leaf-restricted,
94 limiting their use in the field and for broad plant species.

95 The microneedle (MN) is a new technique that has been applied to precision agricultural
96 activities recently (Jung & Jin, 2021, Nagarkar *et al.*, 2020). MN refers to microscopic needles,
97 typically ranging from 150 to 1500 μm in length, 50 to 250 μm in base width and 1 to 25 μm in tip
98 diameter. MNs can be applied to plant tissues to enhance the delivery of essential compounds such
99 as nutrients, metabolites, and agrochemicals, thereby improving plant health and productivity
100 (Faraji Rad, 2023, Ece *et al.*, 2023). A previous example of the MNs in plant delivery is
101 biocompatible silk MNs that were developed for precision delivery of pesticides and essential
102 compounds into plants (Cao *et al.*, 2023, Cao *et al.*, 2020, Han *et al.*, 2025). Even though this silk-
103 based MN provides a new tool to deliver physiologically functional compounds into crops, the
104 source of materials and fabrication process limit its wide applications in large-scale agricultural
105 activities.

106 In our previous study, we developed a different MN system using polyvinyl alcohol (PVA)
107 as the base material (Paul *et al.*, 2021, Paul *et al.*, 2020, Paul *et al.*, 2022). The PVA-based MN
108 effectively isolated genetic molecules (e.g., DNA and RNA) from plant tissues, demonstrating its
109 potential for use in early and in-field crop disease diagnostics (Paul et al., 2020, Paul et al., 2022).
110 More recently, we also applied PVA MNs to crop seeds (e.g., soybeans), and demonstrated its
111 capability for rapid seed DNA extraction for genotyping and whole genome sequencing, a much-
112 simplified trait analysis technology that can greatly speed up the breeding process (Li *et al.*, 2025)

113 In this study, we explored the capability of cost-effective and easy-to-scale-up PVA-MN
114 to deliver small molecules into plant systems. We first observed the diffusion of fluorescent dyes
115 from MN needle tips into tomato stem vascular tissues. Then, we demonstrated the MN-assisted
116 delivery of plant hormone gibberellic acid (GA3) to promote plant growth and restore lateral
117 flowering in Arabidopsis *ft-10* mutants. Finally, we tested the delivery of salicylic acid (SA) to
118 model plant *Nicotiana benthamiana* to inhibit the transportation of tomato spotted wilt virus
119 (TSWV). Together, these results demonstrated PVA-MN's effectiveness in delivering small
120 molecules, particularly plant hormones, to plants. This PVA-MN system holds great promise for
121 future applications in precision agriculture.

122

123 **Results:**

124 **Delivery of fluorescent molecules in plant tissue**

125 PVA (Polyvinyl Alcohol) is a synthetic polymer with several distinct characteristics, such as water
126 solubility, biodegradability, non-toxicity, and tunable mechanical properties, making it a good
127 candidate for applications in plant delivery. To test whether PVA-MN could be applied in chemical
128 delivery in plant tissue, we first applied it to both the leaf and stem of tomato plants. Due to the
129 strong hygroscopic nature of PVA, we observed that leaf tissues punctured by the PVA-MN
130 dehydrated rapidly if the PVA-MN was not removed immediately (e.g., contact time >20 s) after
131 penetration, causing surrounding tissues to wilt within an hour post-puncture (Figure S1). In
132 contrast, when the MN was applied to the stem, although localized dehydration occurred at the
133 puncture site, the vascular bundles remained largely unaffected and continued to function properly
134 (Figure S1). These results indicate that the MN contact time for leaf delivery needs to be controlled,
135 whereas the stem is a more robust delivery site for PVA MNs.

136

137

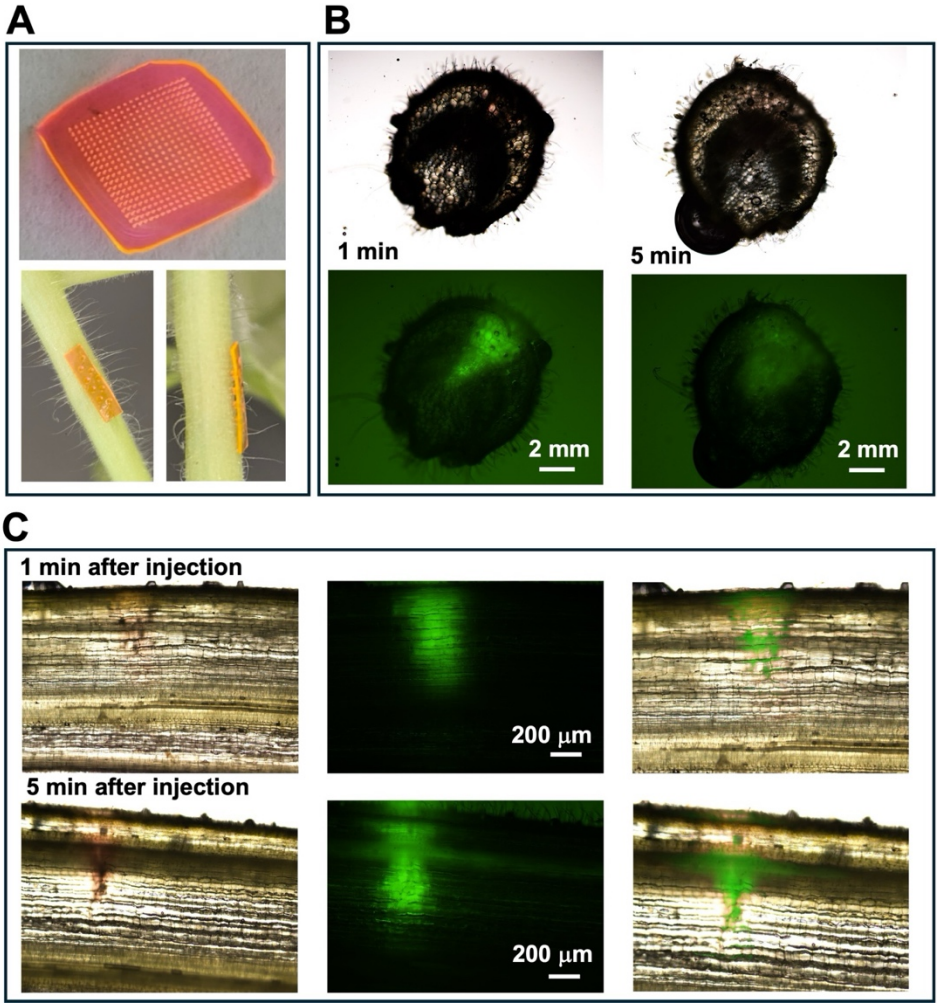

Fig. 1: PVA-MN delivery of fluorescent dyes to tomato plant vasculature system. A. Photographs of rhodamine 6G-loaded PVA MN (top) and a PVA patch loaded with 5(6)-carboxyfluorescein diacetate, inserted into tomato stem (bottom). **B**. Cross-section brightfield and fluorescence microscopy images of the injection site of PVA-MN, depicting that the needle reaches tomato's petiole vasculature system. The loaded dye diffuses out from the needle tip after 1 min and 5 mins of injection. **C.** Vertical-section microscopy images (from left to right: brightfield, fluorescence, and overlap) showing 5(6)-carboxyfluorescein diacetate delivered and transported along xylem, after 1min and 5 min of PVA needle injection.

Tomato was chosen as the model system due to its well-defined vasculature structure and long petioles. Previous studies have shown that the segment between the vasculature and the

150 epidermis ranges from 840–1040 μm for xylem and 707–925 μm for phloem in tomato plants, with
151 xylem and phloem diameters in the tens and hundreds of micrometers, respectively (Cao et al.,
152 2020). Based on these parameters, we designed and fabricated a 1000-μm-long PVA-MN as a
153 microinjector to study payload delivery in planta. We incorporated rhodamine 6G (maximum
154 absorption at 526 nm) and 5(6)-carboxyfluorescein diacetate (maximum absorption at 492 nm) as
155 dye markers into the PVA-MN (Figure 1A). The cross-sectional microscopic images of the petiole
156 confirmed that the 1000 μm MN reached the vascular tissues in the tomato stem (Figure 1B).

157 Using a GFP filter, we observed the diffusion of the 5(6)-carboxyfluorescein diacetate dye
158 into surrounding tissues within 5 minutes of PVA-MN injection (Figure 1B). To analyze molecular
159 transport in the xylem, we performed tangential sectioning of the stem and monitored the dye
160 diffusion at 1-, 5-, and 10-minutes post-injection by fluorescence imaging. The results showed
161 significantly more widespread distribution at 5 minutes post-injection compared to 1 minute
162 (Figure 1C). Quantification of relative fluorescence intensity showed a 32% and 77% increase of
163 dye diffusion area in stems at 5- and 10-minute post-injection, respectively (Figure S2).
164 Additionally, the chemical dyes were observed to travel along the xylem flow in the tomato stem
165 (Figure S3). These findings strongly suggest that the PVA-MN tip effectively reaches the
166 vasculature and that chemical compounds embedded in the PVA-MN can diffuse and be
167 transported along the vascular bundle delivery system in tomato plants.

168

169 **Delivery of growth regulator GA3 to promote tomato plant growth**

170 To demonstrate the utility of PVA-MN to deliver PGRs (Plant Growth Regulators) in crops, we
171 investigated the delivery of gibberellic acid (GA3) to tomato plants. GA3 is a plant hormone that
172 plays a crucial role in regulating various growth and developmental processes in plants, such as
173 seed germination, stem elongation, flowering, and fruit development (Gupta & Chakrabarty, 2013).
174 In the current study, tomato stem was selected as the injection site.

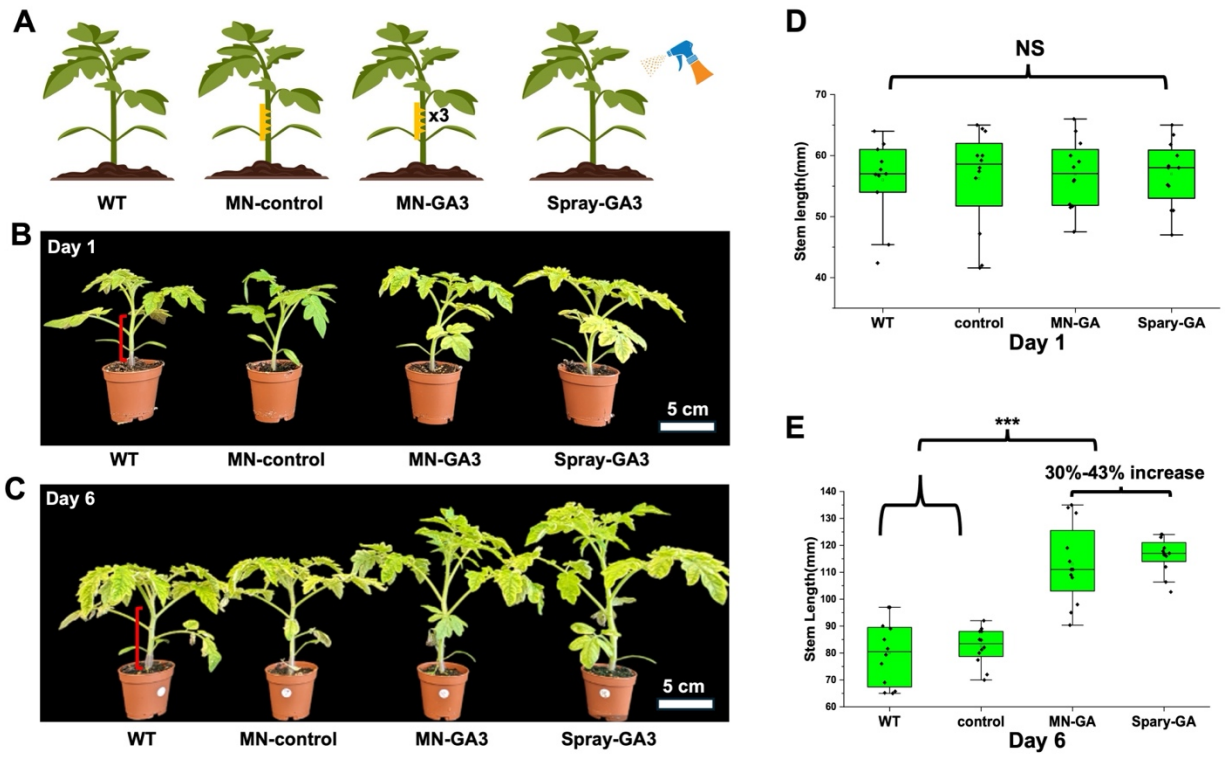

Fig. 2: Tomato phenotype characterization with and without the MN-GA3 (gibberellic acid) treatment. A. Schematic of GA3 treatment model on 25-day-old tomato plants using MN or spray-based delivery methods. **B.** The phenotype of 25-day-old tomato plants after different GA3 treatments. **C.** The phenotype changes of tomato plants (same plants in 2B) 6 days after different GA3 treatments. D. The stem length of the tomato plants at Day 1 after the MN-GA3 and Spray-GA3 treatments (n=12). **E.** The stem length of the tomato plants at Day 6 after the MN-GA3 and Spray-GA3 treatments (n=12).

Twenty-five-day-old tomato plants (n=12) were injected with the PVA-MN-GA on the stem tissue (Figure 2A, Figure S4). Following the initial MN injection, secondary and tertiary injections were performed 3 and 6 days later, respectively. As controls, plants injected with PVA-MN without GA3 (negative control, or "MN-control") and plants sprayed with GA3 on their leaves (positive control, or "Spray-GA3") were included in the experiment (Figure 2A). In addition, healthy plants without any MN or GA3 treatment were used as the wild type ("WT", Figure 2A). The PVA-MN patch contains 500 μM GA3, which is higher than the loading concentration of GA3 in the spray method (100 μM). However, due to the much smaller delivery volume of the PVA-

192 MN method (only an array of ~ 4 x 10 needles touch stems) compared to 5-10 mL of solutions
193 applied in the spray method, three treatments of PVA-MN deliver an estimated total amount of
194 0.05-0.075 μmol of GA3, which is only about 10% of the spray method (Table 1).

195 After six days, we observed that tomato plants treated with MN-GA3 or Spray-GA3
196 exhibited a faster growth rate compared to control plants (both WT and MN-control, Figure 2B,
197 C). Stem lengths (labeled in red, Figure 2B and 2C) were measured at the same time (Figure 2D),
198 revealing that after 3 days, the heights of MN-GA3 and Spray-GA3-treated tomato plants were
199 18%–21% higher than those of the WT or MN-control plants (Figure S4C). After 6 days, GA3-
200 treated plants showed an increase of 30%–43% in height compared to the non-treated controls
201 (Figure 2E). It is noticed that even though the PVA-MN method achieved similar delivery effect
202 compared to conventional spray method (Figure 2E), it showed slightly larger error bars compared
203 to the traditional leaf-spray methods. This may be due to individual differences in the plant and
204 injection location-induced variations of the PVA-MN delivery system.

205 Additionally, GA3 based PVA-MN injection was also performed on the lateral branch by
206 using 40-day-old tomato plants (Figure S5A and S5B). The injection process is the same with the
207 stem treatment. Due to the difference in the initial length of each lateral branch, we calculated the
208 relative lateral branch elongation to evaluate the GA stimulation. The results showed that after 3
209 days of treatment, the average lateral branch of MN-GA3 and Spray-GA3-treated tomato plants
210 grew around 5% more than the WT and MN-control plants (Figure S5C); After 6 days post-
211 injection, the average lateral branch length increased by nearly 10% of control groups (Figure
212 S5D).

213 In addition to stem or branch growth length difference, we also observed that the tomato
214 plants in GA3-treated groups (MN-GA3 and Spray-GA3) showed a noticeable color difference
215 from 4th to 6th compound leaf (newly emerging leaves) (Figure S6A). We assume that this
216 phenotype difference is probably due to the accelerated growth under the GA3 triggering. The
217 concentration of chlorophyll a ($p = 0.0049$) and b ($p = 0.0025$) in the 4th to 6th leaves (mix samples)
218 was quantified. The results showed that in GA3-treated tomato, the leaf chlorophyll a and b content
219 decreased by 6% to 10% compared to the WT and PVA-MN control plants (Figure S6B and S6C).

220 To investigate whether the MN-GA3 treatment would trigger the intrinsic gene
221 transcription level change in tomato plants. We conducted a series of reverse transcription-

quantitative polymerase chain reaction (RT-qPCR) experiments using tomato leaf samples after different treatments. We selected the GA-signal receptor, two tomato *SID* genes (Shohat *et al.*, 2021), as targets and ran the gene expression analysis. The results revealed that after the MN-GA3 or Spray-GA3 treatments, both *SiGID1* and *SiGID1b1* genes showed significant increases in transcription level by 2 to 15-fold compared to the WT and MN-control plants (Figure 3). The expression level of MN-GA3 group is generally comparable to the Spray-GA3 group (Figure 3). Interestingly, in individual plant #9, the MN treatment promoted a higher level of *GID* gene expression than the conventional spraying. All these above data strongly suggest that the PVA-MN-GA injection promotes the stem or branch growth similarly to the foliar spray method, while reducing the application dose by 10~20 times. Consistently, the gene expression involved in the GA signal in tomato plants was also upregulated, confirming the effectiveness of MN delivery of GA into tomato plants.

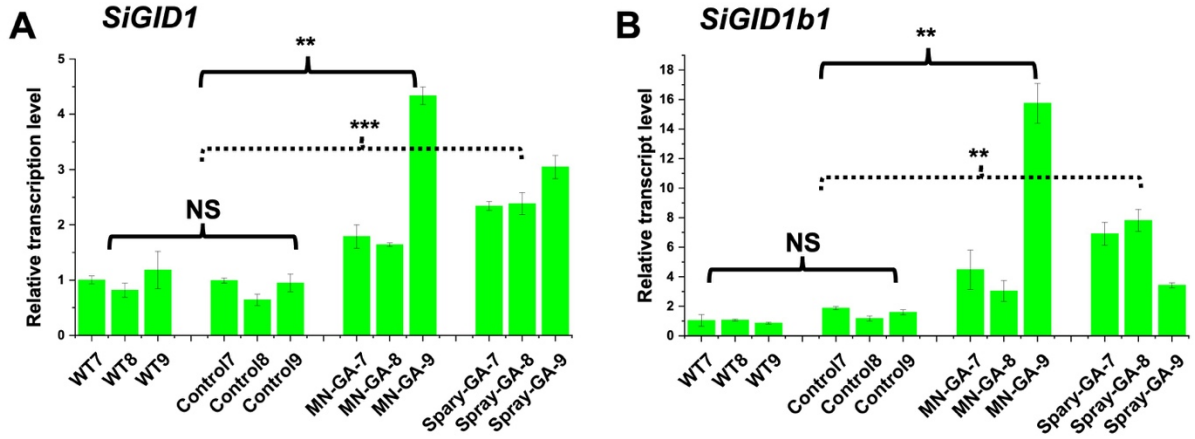

Fig. 3: Tomato gene expression level under different GA stimulations using PVA-MN or GA3 spray. **A**. The relative transcription level change of *SlGID1* genes under the different GA treatments in tomato plants. Each group has three different plant lines (plants 7, 8, 9). **B**. The relative transcription level change of *SlGID1b1* genes under the different GA treatments in tomato plants. Each group has three different plant lines (plants 7, 8, 9). (NS: none significant, *P < 0.05, **P < 0.01, ***P < 0.001)

244 **PVA-MN for GA3 Delivery to *Arabidopsis ft-10 mutant***

245 Besides tomatoes, we also used the model plant *Arabidopsis thaliana* and investigated the PVA-
246 MN injection effects on GA signaling process. *A. thaliana* showed multiple advantages in
247 phenotyping analysis such as well-characterized biological activities, such as development,
248 metabolism, hormone signaling, and stress responses, ease of genetic manipulation, and
249 comprehensive genomic information.

250 Numerous studies have shown that applying gibberellins (such as GA3) in *A. thaliana*
251 promotes the termination of vegetative growth, regulates flower formation, accelerates bolting,
252 and results in plants with fewer rosette leaves and more cauline leaves (Bao *et al.*, 2020). Under
253 normal conditions, wild-type *A. thaliana* Col-0 plants produce around 14 rosette leaves during the
254 vegetative growth phase before inflorescence emergence at approximately 23 days under a 16-
255 hour light regime. Some studies report 11–13 rosette leaves between days 21–24 (Cao et al., 2023).
256 Cao and colleagues studied the *Arabidopsis ft-10* mutant, a *FT* gene loss-of-function mutant with
257 a clear late-flowering phenotype under long-day conditions, to evaluate their silk-based
258 microneedle delivery system (Cao et al., 2023). This mutant disrupts non-GA3-related pathways
259 that predominantly regulate flowering under long-day conditions (Figure S7A). Unlike the
260 previous silk-based microneedles, our study applied PVA-MN to the petiole of a single rosette leaf
261 in *Arabidopsis* plants (Figure S7B, C). The PVA-MN used in this experiment was 800 μm in height.

262 To assess the effectiveness of PVA-MN in delivering GA3 to *Arabidopsis* plants, we
263 compared MN-mediated delivery to foliar spray again. Additionally, an empty PVA-MN (without
264 GA3) was used as a negative control (MN-control, Figure 4A). GA3 was delivered via PVA-MN
265 injections at multiple leaves every 3 days, for a total of three applications, similar to the frequency
266 of foliar sprays. For MN injection on *Arabidopsis* vein, a small array of 2x10 needles were used.
267 The spray method used 2~4 mL GA3 solution instead. The total GA3 amount delivered by the
268 spray method is nearly 10 times of that used in the MN injection methods (Table1).

269

270

271

272 **Table 1. Comparison of plant hormone consumption in different delivery methods**

Plants	Cargo	Delivery Methods		
		MN-GA	Spray-GA	
Tomato	GA	0.05~0.075 μmol	0.5~1 μmol	
Arabidopsis		0.025~0.03 μmol	0.2~0.4 μmol	
		MN-SA	Spray-SA	Infiltration-SA
Nicotine benthamiana	SA	1.2~1.6 μmol	200~250 μmol	50 μmol

273

274 We observed that both Spray-GA and MN-GA treatments resulted in an early bolting
275 phenotype compared to the *ft-10* mutant control and the MN-control (MN only, without GA3)
276 (Figure 4B). Although PVA-MN-GA-treated plants bolted earlier than the controls, their response
277 was slower than that of Spray-GA-treated plants (Figure 4B). Rosette and cauline leaf numbers
278 were also recorded throughout the growth period. GA3-loaded PVA-MN injections produced
279 phenotypes in *ft-10* similar to those observed in GA3 foliar-sprayed plants, with changes in rosette
280 and cauline leaf numbers and leaf size. These phenotypes were significantly different from those
281 *ft-10* mutants untreated with GA3 (Figure 5A). This confirms that GA3 delivered via microneedles
282 effectively altered plant metabolism. Interestingly, MN-control plants (without GA3) produced
283 fewer rosette leaves than the untreated *ft-10* mutant, suggesting that PVA-MN injection may
284 induce some stress even in the absence of GA3 (Figure 5A). These phenotypic findings
285 demonstrate that PVA-MN is effective in delivering GA3 to *Arabidopsis* plants and change their
286 growth behavior accordingly.

287

288

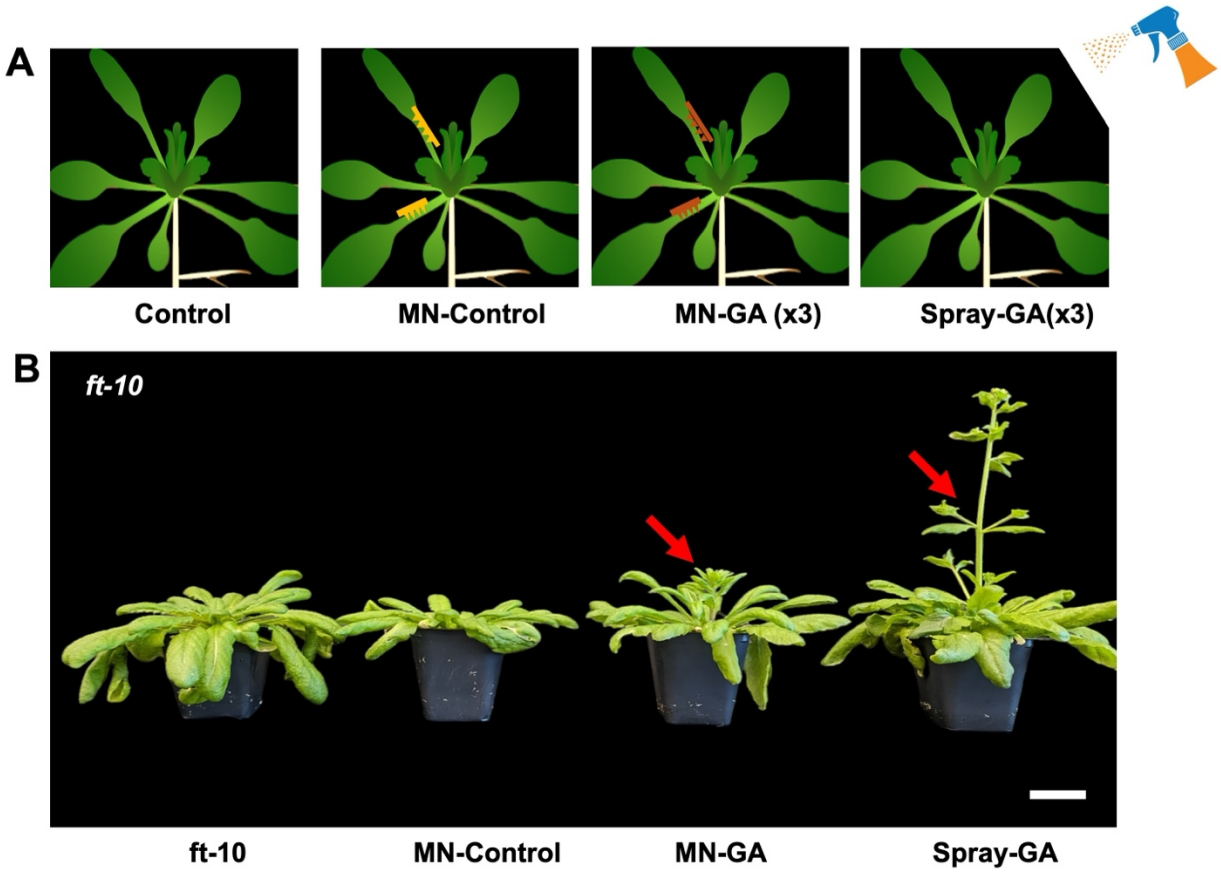

Fig. 4: PVA-MN for GA3 delivery to Arabidopsis *ft-10* mutant. A. Schematic of GA3 delivery to Arabidopsis *ft-10* mutant by PVA-MN and spray methods. **B**. Representative images of *ft-10* plants 10 days after different GA treatments. MN injection and spray were carried out every three days. 4 groups of *ft-10* (n=5 for each group) were treated differently (*ft-10*, MN-control, MN-GA3, Spray-GA3).

In *Arabidopsis* plant, there are three GA receptor isoform genes, namely *AtGID1a*, *1b,* and *1c*. Using RT-qPCR, we analyzed the transcript level of these three genes with and without the PVA-MN-GA3 treatment. We observed that the *AtGID1a* showed a low transcript level in the *Arabidopsis ft-10* mutant background (data not included), but the other two GA receptor genes, the *AtGID1b* and *AtGID1c*, showed a significant increase of the mRNA level by 2 to 10 folds after the MN-GA and Spray-GA treatments (Figure 5B). These molecular results confirm the previous

phenotypic observations, suggesting that PVA-MN is an effective tool for delivering plant hormones in *Arabidopsis*.

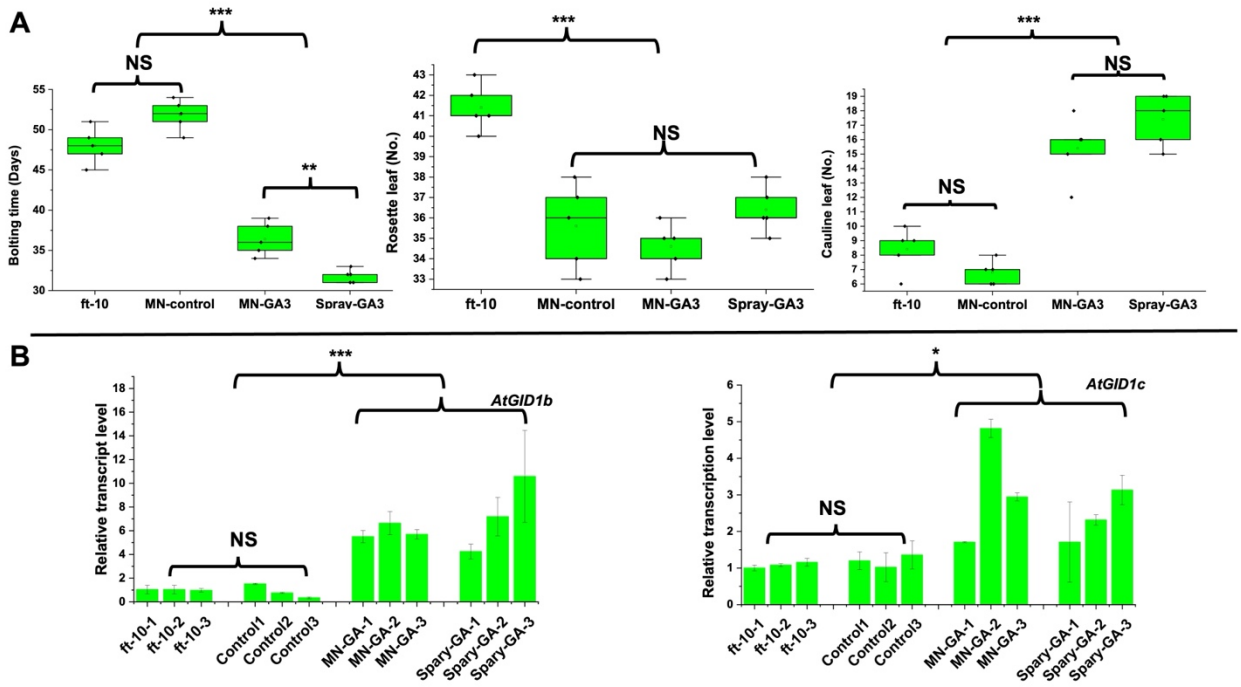

Fig. 5: Different GA delivery treatments change the Arabidopsis phenotype and gene expression in GA signal pathway. A. The bolting time, rosette leaf number, and cauline leaf number change under different GA treatments in Arabidopsis *ft-10* mutants. **B**. The relative transcription level change of *AtGID1b* and *AtGID1c* genes under different GA treatments in tomato plants. Each group has three different plant lines (plants 1, 2, 3). (NS: none significant, *P < 0.05, **P < 0.01, ***P < 0.001)

Delivery of SA for induced TSWV resistance in *Nicotiana benthamiana* plant

Tomato spotted wilt virus (TSWV) is a plant virus that belongs to the family *Tospoviridae* and is one of the most economically significant plant viruses affecting crops worldwide (Best, 1968). The infected plants often show necrotic spots, wilting, chlorosis (yellowing), stunted growth, leaf deformation phenotype, and in some cases, ring spots or concentric patterns on leaves and fruits. These symptoms lead to reduced yield and poor fruit quality. Plant hormone salicylic acid (SA)

has been shown to play a significant role in triggering the resistance response to TSWV in plants (Turina *et al.*, 2016). SA is a crucial plant hormone involved in systemic acquired resistance (SAR), a defense mechanism that provides broad-spectrum resistance to a variety of pathogens, including viruses like TSWV (Durner *et al.*, 1997). In the following experiment, we used PVA-MN to deliver SA directly into plant tissues and investigated whether the MN microinjection could help the model plant *Nicotiana benthamiana* generate resistance to TSWV. Normally, the virus would move within plants through a well-coordinated process that involves both cell-to-cell movement and systemic movement via the plant's vascular system. To monitor TSWV movement in the plant, TSWV infectious clone generated by Liu et al 2023 was engineered. Cas9 in the infectious clone was replaced with RUBY reporter (Liu *et al.*, 2023), which makes the virus' movement visible to naked eye (Figure S8).

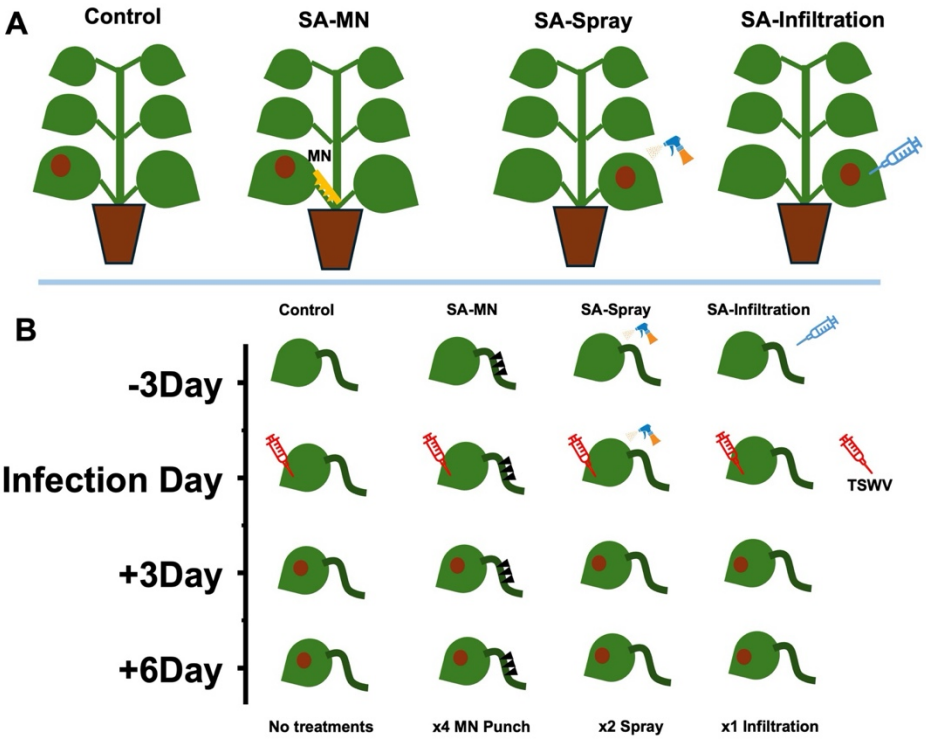

Fig. 6: Schematic showing SA delivery experiments to prevent TSWV virus movement in *Nicotine benthamiana* plants. A. A testing model showing different SA delivery approaches. **B**. A treatment timeline showing the SA treatment process for SA-MN, SA-spray and SA-infiltration in *Nicotine benthamiana* plants.

336 We compared the SA delivery and treatment efficiency of four different methods, including
337 control (no SA delivery), SA-MN, SA-Spray, and SA-infiltration (Figure 6A). For SA-MN, the
338 MN patch loaded with SA was applied to *Nicotiana benthamiana* petiole for 4 times in total (1x
339 before and 3x after TSWV inoculation). The SA-Spray method was performed 2 times (before and
340 after inoculation) and SA-Infiltration method was only performed 1 time on *N. benthamiana*
341 (Figure 6B). For PVA-MN injection on one *Nicotiana benthamiana* plant, a small MN array of
342 4x10 needles was used. The spray and infiltration treatments used 20-25 mL and 8-10 mL of SA
343 solutions, respectively. The absolute amounts of SA delivered to tobacco plants by different
344 delivery methods are summarized in Table 1.

345 Three weeks old *N. benthamiana* plants were used for the experiment. These plants were
346 divided into four groups: 1) control plants, sprayed with water, 2) plants treated with SA-MN, 3)
347 plants sprayed with SA, and 4) plants infiltrated with SA. Seventy-two hours after initial treatments,
348 all these plants were agro-infiltrated with TSWV infectious clone. Post infection MN-SA group
349 received the second SA-MN treatment, and SA sprayed group received the second SA treatment.
350 Subsequently, the SA-MN group was treated two more times, on day 6 and day 9, totaling four
351 SA-MN applications. The SA spray group received two treatments in total, while the SA
352 infiltration group was treated only once (Figure 6B).

353 In the first trial, the SA-MN group applied 2 mM SA, while the SA-Spray and SA-
354 Infiltration groups used only 500 μM SA, given their larger application volumes. Still, the
355 estimated amount of SA delivered to the plants by the MN approach is only about 0.5-1% of the
356 spray or infiltration method (Table 1). Three days after inoculation of *N. benthamiana* plants with
357 TSWV, we observed the virus infection in all test groups as evident by the expression of RUBY
358 (red color). We found that nearly 67% of the infected leaves on control plants (without SA
359 treatment) turned dark red color. However, only about 20% of the leaves showed dark color in SA-
360 treated plants (Figure 7A). Also, no major differences were observed between SA-MN, SA-Spray,
361 and SA-infiltration groups. After 6 days, nearly 92% of the infected leaves were dark red in the
362 control plants. At the same time, the percentage of dark red color in SA-treated groups was kept
363 lower at around 50% (Figure 7A). In Figure 7A, the dark color indicates more RUBY expression
364 thus more viral load, whereas light color indicates less viral load. These results suggest that the
365 SA treatment inhibited TSWV infection.

366 This indicates MN is a highly effective delivery platform for sending SA into leaf tissues
367 and inducing TSWV resistance. It is also interesting to note that after 15 days of viral infection,
368 all the infected leaves demonstrated a dark red color and died due to virus infection. The petioles
369 of control, SA-Spray and SA-infiltration groups all turned red color (Figure 7B), indicating the
370 transportation of TSWV along the plant vasculature system. However, the SA-MN treated petiole
371 remained green (Figure 7B), indicating a strong viral resistance and fewer viral transportation in
372 the SA-MN treated petiole tissue.

373 The comparison experiments were repeated by increasing the concentration of SA in SA-
374 Spray and SA-infiltration methods to 1 mM instead of 500 μM (Figure S9A). After 20 days of
375 infection, the control group clearly showed that the movement of TSWV from the leaf tissue to
376 the stem, along the vein in the WT *Nicotina benthamiana* plants (Figure S9B). However, in SA-
377 MN, SA-Spray, and SA-infiltrated plants, no red color on the stem was observed (Figure S9B).
378 After 30 days of infection, the control plant revealed a dwarf phenotype compared to the SA-
379 treated plants (Figure S10A). The stem of control plants showed tissue wilting. On the contrary,
380 the SA-MN and SA-Spray treated plants were still healthy, while some viral infection (red color)
381 was also found in SA-infiltrated plants (Figure S10B), which may be due to less total SA treatment
382 dose in the infiltration method (infiltration: 5 mL of 1 mM SA; Spray: 10 mL of 1 mM SA and
383 repeated 2x).

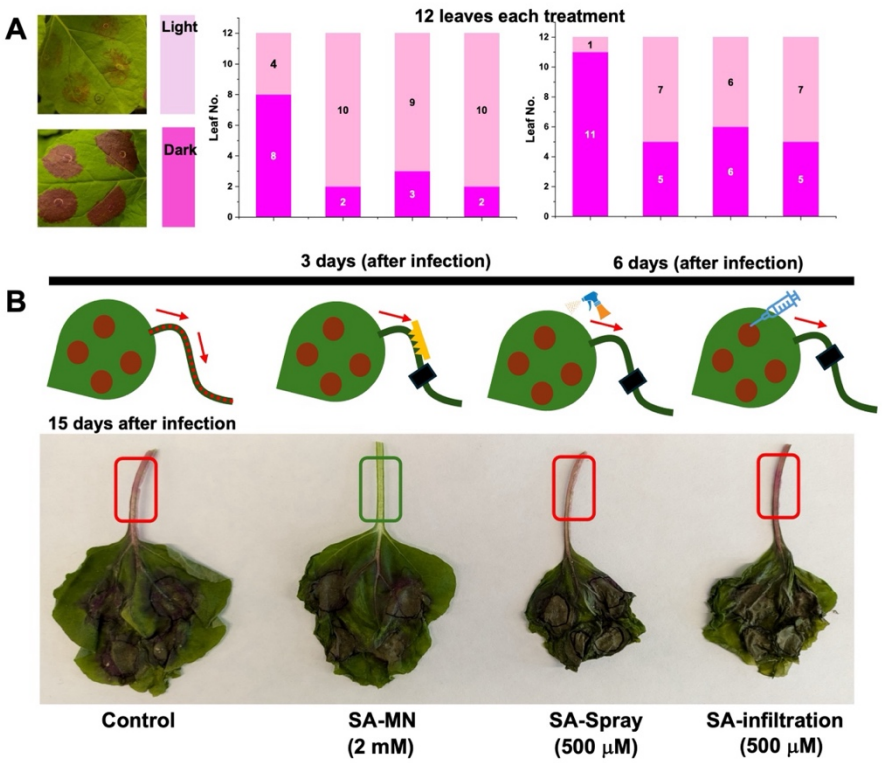

Fig. 7: SA-MN delivery prevents TSWV movement in *Nicotine Benthamiana*. A. TSWV infection in *N. benthamiana* leaf after SA treatments at 3 days and 6 days, respectively as evident by the expression of RUBY. The light red color indicated less TSWV infection, while the dark red color indicated higher TSWV load. **B**. The phenotype of TSWV infected-*Nicotine benthamiana* (15 days post infection). SA-MN delivery inhibited the TSWV movement from the leaf to petiole.

These experiments strongly suggested that the SA could be effectively delivered to *Nicotiana benthamiana* plants by the MN delivery method and induce resistance to TSWV infection. Compared to the traditional spray method, although the SA-MN method is more frequent (total four times) and has a higher SA concentration (2 mM), it significantly reduces the total application dose by ~99% (Table 1) while achieving similar immunization effects. Moreover, the spray method required multiple treatment positions, including the applications to adaxial and the abaxial sides of the leaf, while the PVA-MN injection simply works on the stem or petiole. This

399 suggests that our PVA-MN delivery method uses less active ingredient and also a faster application
400 method.

401

402 **Discussion**

403 In this study, we demonstrated that PVA MN patches could be effectively utilized as a precision
404 plant delivery system for various compounds, including small-molecule dyes, growth hormones,
405 and antiviral agents (Figure 8). Compared to conventional delivery methods such as foliar spray
406 and soil application, which suffer from high chemical losses, environmental impact, and low
407 absorption, PVA-MNs offer a promising alternative that can directly target plant tissues with high
408 precision and reduced application dose and environmental side effects. Our results showed that the
409 PVA-MNs successfully delivered fluorescent dyes into the vascular tissues of tomato stems,
410 confirming the capability of these MNs to penetrate plant tissues and facilitate compound diffusion.
411 This is significant as it highlights the unique advantage of PVA-MNs to enhance the uptake and
412 transport of bioactive molecules within plants, addressing a critical limitation of foliar and soil
413 applications, where the efficacy of nutrient and agrochemical delivery is compromised by
414 environmental factors and the natural barriers of plant surfaces.

415

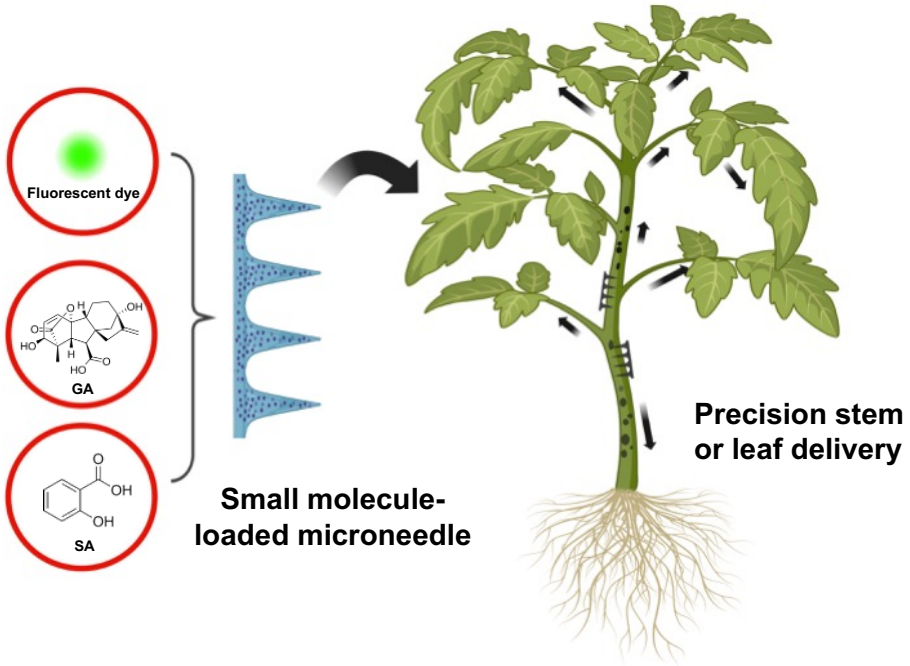

Fig. 8: Schematic of PVA microneedle delivery platform for delivering different cargos into a live plant.

The delivery of GA3 through PVA-MNs in tomato plants resulted in accelerated stem growth and an altered chlorophyll profile in newly emerged leaves, indicating effective hormone delivery and physiological response. Compared to traditional foliar spray methods, MNs demonstrated similar or slightly enhanced growth-promoting effects while reducing application amount of GA3 by nearly 90%, suggesting that PVA-MNs is a more controlled and sustained delivery method. The transcriptional upregulation of GA receptor genes further supports the successful delivery of GA3, confirming that MNs can effectively trigger hormonal signaling pathways in planta. In *Arabidopsis ft-10* mutants, known for their delayed flowering phenotype, PVA-MN-mediated GA3 delivery induced earlier bolting, resembling the phenotypic response seen with foliar sprays. This response validates the use of MNs for delivering hormones in a model plant system and emphasizes their potential utility in precision agriculture to manipulate plant growth and development. The observed upregulation of GA receptor genes in treated plants

underscores the ability of PVA-MNs to modulate gene expression and drive desired phenotypic outcomes.

Finally, the application of SA via PVA-MNs in *N. benthamiana* demonstrated the MN's ability to enhance plant resistance against TSWV, a new way of plant immunization with high accuracy. The restricted movement of the virus in SA-treated plants highlights the effectiveness of MNs in delivering antiviral compounds directly to the infection site, enhancing the plant's natural defense mechanisms. This approach offers a targeted method to combat viral infections, potentially reducing the need for broad-spectrum chemical treatments that can harm the environment.

Despite these promising results, several challenges remain to in implementing MN-based delivery methods in future. For instance, the dehydration effect observed in MN-treated leaf tissues suggests that MN application may be more suitable for stems or thicker plant parts where the tissue is more robust. Stem delivery may potentially also accept a larger amount of payloads and transport the delivered payloads faster to other parts of the plant than leaf delivery. Additionally, while MNs provide a more direct and potentially more efficient delivery option, the injection process could be further automated in future (e.g., use of robotic arms) to scale up the process and minimize tissue damage by more controlled pressure application.

Overall, our findings suggest that PVA-MNs are a viable and effective tool for plant compound delivery, offering benefits over traditional methods in terms of precision, efficiency, and reduced environmental impact. Future research should focus on scaling up MN fabrication processes, automating delivery techniques, and expanding the range of compounds that can be effectively delivered through this innovative system. With continued development, MN delivery technology could potentially revolutionize precision agriculture, enabling more sustainable and targeted interventions in crop management.

457 **Materials and methods:**

458 **Plant materials and growing conditions**

459 Arabidopsis thaliana *ft-10* mutant seeds (TAIR Germplasm CS9869) and ecotype Columbia (Col-
460 0) seeds were sterilized by soaking for 1 min in 70% ethanol and then for 10 min in 20% bleach,
461 followed by five to seven rinsing with sterile distilled water. Sterilized seeds were placed on
462 Murashige and Skoog (MS) plates and kept at 4 °C for 2 days. The plate was placed in a plant
463 growth chamber (Caron 7304-22-1) at 22 °C with long day (day/night 16h/8h) conditions, 70–100%
464 relative humidity, and light intensity of 100 μmol m^{-2} s^{-1}. Seedlings were transferred to pots (2.5
465 × 2.5 × 3 in^3) with soil (Miracle-Gro Moisture Control Potting Soil Mix) on day 7 and watered
466 regularly. Tomato (*Solanum lycopersicum* var. Beefsteak) seeds were purchased from The Seed
467 Plant. Tomato seeds were grown in pots (3.5 × 3.5 × 3 in^3) in the plant room under long day
468 (day/night 16h/8h) at 80 μmol m^{-2} s^{-1}, 70–90% relative humidity, day and night temperatures of
469 26 and 20 °C, respectively. *Nicotiana benthamiana* plants were grown in the growth chamber at
470 12h day and 12h night at 26°C at 275 μmol m^{-2} s^{-1}.

471 **TSWV virus infection**

472 *Agrobacterium tumefaciens* GV3101 carrying recombinant plasmids (pL, pM-RUBY, pS-NSs,
473 and triple VSR (viral suppressor of RNAi) were grown in Luria Broth media containing
474 appropriate antibiotics (Rifampicin (50 μg/ml), Kanamycin (50 μg/ml), and Gentamycin
475 (50 μg/ml)) for overnight. Cells were harvested from overnight grown cultures of *Agrobacterium*
476 and re-suspended into the infiltration buffer (10 mM $MgCl_2$, 10 mM MES pH 5.6 and 100 μM
477 acetosyringone) at OD600 of 1, and further incubated at 28ºC for 3 hours. Before infiltration,
478 *Agrobacterium* cultures carrying pL, pM-RUBY, pS-NSs, and triple VSR plasmids were mixed at
479 final OD600 of 0.25. Three hours post-incubation, fully expanded *Nicotiana benthamiana* leaves
480 were co-infiltrated with *Agrobacterium* cells harboring pL, pM-RUBY, pS-NSs, and triple VSR
481 plasmids at final OD600 of 0.25 (Liu et al., 2023).

482 **PVA MN fabrication process**

483 The microneedle patch was fabricated using a simple centrifugation method using
484 polydimethylsiloxanes (PDMS)-based negative molds (Blueacre Technology) in a 10 (w/v) %

485 polyvinyl alcohol (PVA) (M.W. 31,000-50,000, 98.0-98.8% hydrolyzed) (Acros Organics)
486 solution. To remove dust and debris from the micron-scale crevices of the PDMS molds, each chip
487 is first cleaned by repeated rinses with deionized (DI) water followed by two rounds of sonication
488 for 5 minutes each. The molds then dried at 35°C for 10-20 minutes to evaporate any remaining
489 water droplets clinging onto the needle edges. Next, 1.2 mL of PVA is allotted in 1.7 mL centrifuge
490 tubes which undergo their first round of centrifugation at 7500 rpm (Fisher Scientific accuSpin
491 Micro17) for 10 minutes without the mold to remove any trapped air bubbles. The molds are then
492 submerged into these tubes with the needle molds facing inwards and centrifuged again at 7500
493 rpm for 10 minutes to facilitate PVA flow into the holes. The molds are then removed and sealed
494 with another layer of PVA to allow the formation of a stronger base for the needles upon drying.
495 Lastly, the MN patches are partially covered (for slow evaporation) and cured for 24 hours at room
496 temperature to allow complete solidification.

497 *MN patch fabrication with Gibberellic acid (GA3):* 34.6 mg of GA3 is dissolved in 500 µL
498 of dimethylsulfoxide (DMSO) and 500 µL of deionized (DI) water to make a stock solution of 100
499 mM of GA3. 6 µL of the solution is added to 1.2 mL of 10 (w/v) % PVA solution to make a final
500 GA3 concentration of 500 µM in 10 (w/v) % PVA solution for one microneedle patch. Each 20 x
501 20 MN array is made from 500 µL PVA-GA3 solution. In the tomato treatment experiments, only
502 a 4 x 10 array was pressed to the plant stem due to the small size of plant stems. The estimated
503 amounts of total GA3 delivered to different plants by MN are summarized in Table 1.

504 *MN patch fabrication with Salicylic Acid (SA):* 11.04 mg of SA is dissolved in 15 mL of
505 DI water to make a stock solution of 5.33 mM. This solution is then added to 16 (w/v) % PVA
506 solution to make a final solution of 2 mM SA and 10% (w/v) PVA for microneedle fabrication.

507 *MN patch fabrication with Rhodamine and 5(6)-carboxyfluorescein (5(6)-FAM):* 52 mg of
508 Rhodamine is dissolved in 1.2 mL DI water to make a stock solution of 0.0905 M. On the other
509 hand, to make a stock solution of 0.2715 M 5(6)-FAM, 25 mg of the powder is dissolved in 200
510 µL of DMSO. 33 µL and 11 µL of the respective stock solutions were added to 30 mL of 10 (w/v) %
511 PVA to make a final solution containing 0.1 mM of Rhodamine and 5(6)-FAM each that was used
512 to fabricate the microneedles.

513

514 **Fluorescent dye delivery in tomato plants**

515 5(6)-carboxyfluorescein diacetate (1 mM) and rhodamine 6G (1 mM) were mixed with a DMSO
516 solution at a volume ratio of 1:100 when fabricating the PVA-MN. To monitor fluorescence signal
517 from the delivery and transport of 5(6)-carboxyfluorescein diacetate and rhodamine 6G, cross-
518 sections upstream and downstream along the petiole were observed under a microscope with fixed
519 light intensity and an exposure time of 20 ms. The petiole was also sliced longitudinally to image
520 the distribution profile of 5(6)-carboxyfluorescein diacetate in the xylem. Image analysis was
521 performed using ImageJ 1.52i. Fluorescence intensity was used as a proxy for the concentration of
522 5(6)-carboxyfluorescein diacetate within the tested range, and fluorescence signals were integrated
523 radially.

524 **Plant hormone preparation**

525 GA3 Solution Preparation: 0.1 M stock solution of GA3 was prepared by dissolving 34.6 mg GA3
526 in 1 mL 75% ethanol solution. GA3 spray solution was prepared by diluting stock solution 1000×
527 to a final concentration of 100μM. Silwet-77 was added to obtain a final concentration of 0.01%
528 in the GA3 spray.

529 SA Solution Preparation: 100 mM stock solution of SA was prepared by dissolving 138
530 mg SA in 1 mL 75% ethanol solution. The SA spray solution was prepared by diluting 100 mM
531 SA stock 1000X to the final concentration of 0.1×10^{-3} M. Tween-20 was added to obtain a final
532 concentration of 0.01% in the SA spray and used as a surfactant to promote SA absorption.

533 **QRT-PCR based gene expression analysis**

534 Quantitative RT-PCR analysis was performed using SYBR-Green PCR Master mix (Invitrogen,
535 Carlsbad, CA, United States) on a CFX96TM (Bio-Rad, California, CA, United States). Gene-
536 specific primer pairs and different thermal programs (Supplementary Table S1) were developed to
537 compare expression levels in *Arabidopsis*, tomato, and *N. benthamiana* plants. Arabidopsis
538 *UBQ10* gene and tomato Actin gene were used as reference controls for normalization. Amplified
539 products were monitored using an optical reaction module (SYBR-green) and the resulting
540 amplified values of genes were normalized against those of references according to a previous
541 protocol for plants (Li *et al.*, 2021). Steps of PCR analysis were carried out following the method
542 described previously (Li et al., 2021). The reaction system was composed of 12 μL mixture,

543 including: 10 μL of SYBR-green-preMix, 1.0 μL of 10 μM forward and reverse primer, and 1.0
544 μL of cDNA template(Li *et al.*, 2017). The thermal program followed the protocol of Bio-rad
545 SYBR-Green PCR Master-mix. The thermal program is 95 ºC for 30s, (95 ºC for 10s, 60 ºC for 1
546 min) ×40, 65 ºC to 95 ºC with 0.5 ºC increments in 2s, 4 ºC. Three replicates were performed in
547 this assay for each gene expression analysis. All the primers were listed in Supplementary Table
548 S1.

549

550

551

552 **Funding:** The authors sincerely thank the funding support provided by Kenan Institute and the
553 Game-Changing Research Incentive Program for the Plant Sciences Initiative (GRIP4PSI).

554

555

556 **Author Contribution:**

557 M.L. contributed to experiment design, plant treatments, RNA extraction, analysis of all
558 experimental data, figure preparation, and manuscript drafting. A.D.P. contributed to PVA-MN
559 preparation. D.S. and A.E.W. helped construct the RUBY-TSWV and TSWV infection
560 experiments. Q.W. perceived and designed the project, developed experimental plans, supervised
561 data analysis, and figure preparation. All authors contributed to the revision of the manuscript.

562

563

564 **Acknowledgements:**

565 The authors thank Dr. Hongwei Jing and Dr. Wusheng Liu at NC State Department of Horticulture
566 for helping with RNA extraction.

Declaration of interests:

The authors declare that the research was conducted in the absence of any commercial or financial relationships that could be construed as a potential conflict of interest.

Reference:

Alkharabsheh, H. M., Seleiman, M. F., Battaglia, M. L., Shami, A., Jalal, R. S., Alhammad, B. A.*, et al.* (2021) Biochar and its broad impacts in soil quality and fertility, nutrient leaching and crop productivity: A review. *Agronomy,* **11,** 993.

Bao, S., Hua, C., Shen, L. and Yu, H. (2020) New insights into gibberellin signaling in regulating flowering in Arabidopsis. *Journal of Integrative Plant Biology,* **62,** 118-131.

Barłóg, P., Grzebisz, W. and Łukowiak, R. (2022) Fertilizers and fertilization strategies mitigating soil factors constraining efficiency of nitrogen in plant production. *Plants,* **11,** 1855.

Beig, B., Niazi, M. B. K., Sher, F., Jahan, Z., Malik, U. S., Khan, M. D.*, et al.* (2022) Nanotechnology-based controlled release of sustainable fertilizers. A review. *Environmental Chemistry Letters,* **20,** 2709-2726.

Best, R. J. (1968) Tomato spotted wilt virus. *Advances in virus research,* **13,** 65-146.

Brichi, L., Fernandes, J. V., Silva, B. M., Vizú, J. d. F., Junior, J. N. and Cherubin, M. R. (2023) Organic residues and their impact on soil health, crop production and sustainable agriculture: A review including bibliographic analysis. *Soil Use and Management,* **39,** 686-706.

Cao, Y., Koh, S. S., Han, Y., Tan, J. J., Kim, D., Chua, N. H.*, et al.* (2023) Drug delivery in plants using silk microneedles. *Advanced Materials,* **35,** 2205794.

Cao, Y., Lim, E., Xu, M., Weng, J. K. and Marelli, B. (2020) Precision delivery of multiscale payloads to tissue-specific targets in plants. *Advanced Science,* **7,** 1903551.

Cunningham, F. J., Goh, N. S., Demirer, G. S., Matos, J. L. and Landry, M. P. (2018) Nanoparticle-mediated delivery towards advancing plant genetic engineering. *Trends in biotechnology,* **36,** 882-897.

Davis, K. F., Gephart, J. A., Emery, K. A., Leach, A. M., Galloway, J. N. and D'Odorico, P. (2016) Meeting future food demand with current agricultural resources. *Global Environmental Change,* **39,** 125-132.

Dimkpa, C. O., Fugice, J., Singh, U. and Lewis, T. D. (2020) Development of fertilizers for enhanced nitrogen use efficiency–Trends and perspectives. *Science of the Total Environment,* **731,** 139113.

Durner, J., Shah, J. and Klessig, D. F. (1997) Salicylic acid and disease resistance in plants. *Trends in plant Science,* **2,** 266-274.

Ece, E., Eş, I. and Inci, F. (2023) Microneedle technology as a new standpoint in agriculture: Treatment and sensing. *Materials Today*.

Faraji Rad, Z. (2023) Microneedle technologies for food and crop health: recent advances and future perspectives. *Advanced Engineering Materials,* **25,** 2201194.

Fukase, E. and Martin, W. (2020) Economic growth, convergence, and world food demand and supply. *World Development,* **132,** 104954.

Gupta, R. and Chakrabarty, S. (2013) Gibberellic acid in plant: still a mystery unresolved. *Plant signaling & behavior,* **8,** e25504.

Han, Y., Jangir, M., Ngoh, A. S. Y., Li, C., Sarangapani, S., Cao, Y.*, et al.* (2025) Precise Delivery of Physiological Doses of Melatonin in Planta to Control Postharvest Physiology and Extend Shelf Life Outside the Cold Chain. *Nano Letters*.

Ishfaq, M., Kiran, A., ur Rehman, H., Farooq, M., Ijaz, N. H., Nadeem, F.*, et al.* (2022) Foliar nutrition: Potential and challenges under multifaceted agriculture. *Environmental and Experimental Botany,* **200,** 104909.

Jakhar, A. M., Aziz, I., Kaleri, A. R., Hasnain, M., Haider, G., Ma, J.*, et al.* (2022) Nano-fertilizers: A sustainable technology for improving crop nutrition and food security. *NanoImpact,* **27,** 100411.

Jung, J. H. and Jin, S. G. (2021) Microneedle for transdermal drug delivery: current trends and fabrication. *Journal of pharmaceutical investigation***,** 1-15.

Krishnasree, R., Raj, S. K. and Chacko, S. R. (2021) Foliar nutrition in vegetables: A review. *Journal of Pharmacognosy and Phytochemistry,* **10,** 2393-2398.

Li, M., Dey, P. A., Cui, Q., Hsieh, T.-F., Summeetha, J., Xu, J.*, et al.* (2025) **Non-destructive seed genotyping via microneedle-basedDNA extraction**. *Plant Biotecnology Journal*.

Li, M., He, X., La Hovary, C., Zhu, Y., Dong, Y., Liu, S.*, et al.* (2021) A De Novo regulation design shows an effectiveness in altering plant secondary metabolism. *Journal of Advanced Research*.

Li, M., Li, Y., Guo, L., Gong, N., Pang, Y., Jiang, W.*, et al.* (2017) Functional characterization of tea (Camellia sinensis) MYB4a transcription factor using an integrative approach. *Frontiers in Plant Science,* **8,** 943.

Liu, C., Zhou, H. and Zhou, J. (2021) The applications of nanotechnology in crop production. *Molecules,* **26,** 7070.

Liu, Q., Zhao, C., Sun, K., Deng, Y. and Li, Z. (2023) Engineered biocontainable RNA virus vectors for non-transgenic genome editing across crop species and genotypes. *Molecular Plant,* **16,** 616-631.

Nagarkar, R., Singh, M., Nguyen, H. X. and Jonnalagadda, S. (2020) A review of recent advances in microneedle technology for transdermal drug delivery. *Journal of Drug Delivery Science and Technology,* **59,** 101923.

Nair, R., Varghese, S. H., Nair, B. G., Maekawa, T., Yoshida, Y. and Kumar, D. S. (2010) Nanoparticulate material delivery to plants. *Plant science,* **179,** 154-163.

Niu, J., Liu, C., Huang, M., Liu, K. and Yan, D. (2021) Effects of foliar fertilization: a review of current status and future perspectives. *Journal of Soil Science and Plant Nutrition,* **21,** 104-118.

Nkebiwe, P. M., Weinmann, M., Bar-Tal, A. and Müller, T. (2016) Fertilizer placement to improve crop nutrient acquisition and yield: A review and meta-analysis. *Field crops research,* **196,** 389-401.

Pahalvi, H. N., Rafiya, L., Rashid, S., Nisar, B. and Kamili, A. N. (2021) Chemical fertilizers and their impact on soil health. *Microbiota and Biofertilizers, Vol 2: Ecofriendly tools for reclamation of degraded soil environs***,** 1-20.

Paul, R., Ostermann, E., Chen, Y., Saville, A. C., Yang, Y., Gu, Z.*, et al.* (2021) Integrated microneedle-smartphone nucleic acid amplification platform for in-field diagnosis of plant diseases. *Biosensors and Bioelectronics,* **187,** 113312.

Paul, R., Ostermann, E. and Wei, Q. (2020) Advances in point-of-care nucleic acid extraction technologies for rapid diagnosis of human and plant diseases. *Biosensors and Bioelectronics,* **169,** 112592.

Paul, R., Ostermann, E. and Wei, Q. (2022) Rapid Extraction of Plant Nucleic Acids by Microneedle Patch for In-Field Detection of Plant Pathogens. In: *Plant Pathology: Method and Protocols*. Springer, pp. 77-90.

Salama, D. M., Abd El-Aziz, M., Rizk, F. A. and Abd Elwahed, M. (2021) Applications of nanotechnology on vegetable crops. *Chemosphere,* **266,** 129026.

Shohat, H., Eliaz, N. I. and Weiss, D. (2021) Gibberellin in tomato: Metabolism, signaling and role in drought responses. *Molecular Horticulture,* **1,** 15.

Sinha, E., Calvin, K. V., Kyle, P. G., Hejazi, M. I., Waldhoff, S. T., Huang, M.*, et al.* (2022) Implication of imposing fertilizer limitations on energy, agriculture, and land systems. *Journal of environmental management,* **305,** 114391.

Tudi, M., Daniel Ruan, H., Wang, L., Lyu, J., Sadler, R., Connell, D.*, et al.* (2021) Agriculture development, pesticide application and its impact on the environment. *International journal of environmental research and public health,* **18,** 1112.

Turina, M., Kormelink, R. and Resende, R. O. (2016) Resistance to tospoviruses in vegetable crops: epidemiological and molecular aspects. *Annual review of phytopathology,* **54,** 347-371.

Tyagi, J., Ahmad, S. and Malik, M. (2022) Nitrogenous fertilizers: Impact on environment sustainability, mitigation strategies, and challenges. *International Journal of Environmental Science and Technology,* **19,** 11649-11672.

Vasundhara, D. and Chhabra, V. (2021) Foliar nutrition in cereals: A review. *Pharma Innov J,* **10,** 1247-1254.

Wang, J. W., Cunningham, F. J., Goh, N. S., Boozarpour, N. N., Pham, M. and Landry, M. P. (2021) Nanoparticles for protein delivery in planta. *Current opinion in plant biology,* **60,** 102052.

Yahaya, S. M., Mahmud, A. A., Abdullahi, M. and Haruna, A. (2023) Recent advances in the chemistry of nitrogen, phosphorus and potassium as fertilizers in soil: a review. *Pedosphere,* **33,** 385-406.

Young, M. D., Ros, G. H. and de Vries, W. (2021) Impacts of agronomic measures on crop, soil, and environmental indicators: A review and synthesis of meta-analysis. *Agriculture, Ecosystems & Environment,* **319,** 107551.

Zhang, H., Cao, Y., Xu, D., Goh, N. S., Demirer, G. S., Cestellos-Blanco, S.*, et al.* (2021) Gold-nanocluster-mediated delivery of siRNA to intact plant cells for efficient gene knockdown. *Nano letters,* **21,** 5859-5866.

Zhang, H., Goh, N. S., Wang, J. W., Pinals, R. L., González-Grandío, E., Demirer, G. S.*, et al.* (2022) Nanoparticle cellular internalization is not required for RNA delivery to mature plant leaves. *Nature nanotechnology,* **17,** 197-205.

Zhang, H., Zhang, H., Demirer, G. S., González-Grandío, E., Fan, C. and Landry, M. P. (2020) Engineering DNA nanostructures for siRNA delivery in plants. *Nature protocols,* **15,** 3064-3087.

Zheng, L., Chen, H., Wang, Y., Mao, Q., Zheng, M., Su, Y.*, et al.* (2020) Responses of soil microbial resource limitation to multiple fertilization strategies. *Soil and Tillage Research,* **196,** 104474.